CENTRE NATIONAL DE LA RECHERCHE SCIENTIFIQUE

UNIVERSITE JOSEPH FOURIER SCIENCES TECHNOLOGIE MEDECINE

LGIT Grenoble

Recosy

Deliverable 3.1

RECOSY

Synthesis and characterization of Solids to be used in WP3

Compiled by

Laurent Charlet, WP 3 Leader

Partners of WP3 are given below. The * denotes groups which have provided information to the WP leader for Deliverable 3.1

1-FZK-INE, 3-BRGM*, 6-CTM*, 7-AMPHOS*, 8-FZD, 14-TUG, 16-CNRS*, 17-UNIZAR, 19-II-HAS*, 20-UCYPRUS*, 22-UNIUTR*, 24-MICANS, 26-GEOPOINT.

1. Redox response of defined and near-natural systems: WP3

1.1. OBJECTIVES

- Quantification and development of process understanding for redox buffer capacity
- Kinetics of response to redox perturbations of defined and near-natural systems..
- Determination of key electrochemical parameters of electrodes
- Redox response of defined and near-natural systems to redox disturbance (i) finely ground COX materials, ii) ions naturally present in the porewater (e.g. H^+, SO_4^{2-}, HS^-, Fe^{2+}), iii) redox sensitive radionuclides analogues (e.g. Se(VI), Se(IV), I^-, CH_4 for ^{14}C) and iv) gases (O_2, CO_2, H_2, H_2S), in different situations, both similar to the expected natural situations and to very perturbed conditions.

1.2. REPOSITORY SYSTEM RELEVANCE

- Near-field: bentonite, argilite
- Far-field. Type of host-rock: clay

1.3. TYPE OF STUDIES

- Laboratory experiments
- Theoretical/modelling of electrochemical behaviour of solids.

1.4. TYPE OF SYSTEM STUDIED

- Heterogeneous

1.2 Type of sample(s) And characterisation: natural, synthetic, Commercial and mineral and metallic samples

1.2.1 Carbonates

- ***Fe(II) doped Calcite (Partner 16)***

Synthesis

A calcite stock suspension of 1.5-1.8 μm average-sized particles was specially prepared according to Mettler et al. (2009). Commercially available calcite (Merck, suprapur; mean particle size ca. 80 μm) was milled in suspension in a zircon oxide ball mill. The milled product was then suspended in $CaCO_3$ saturated water to a concentration of 100.7 g L^{-1}. It served as stock suspension and was kept under atmospheric CO_2 partial pressure. Size distribution of the particles was measured after the milling procedure as well as over the course of the experiments by laser diffraction (Malvern Master Sizer X) to verify that grinding by the stir bar did not occur. No measurable changes were observed during the 8 months of experimentation. The specific surface area of the dried solids was 2.4 m2 g^{-1}, as determined by N_2–BET adsorption. A 1 g L^{-1} calcite suspension was then reacted with 10 μM Fe(II) for 15 hours to 1 week, after which, dissolved and total Fe(II) were measured

Characterization

The $CaCO_3$ solid was characterized by X-ray diffraction measurements (XRD; Scintag XDS 2000, Cu*K*α) as well as ATR infrared spectroscopy (Spectrometer FTS 575C, Bio Rad). The Fe(II)-$CaCO_3$ co-precipitate was further investigated by dissolution with carbonic acid. First Fe(II)-$CaCO_3$ was synthesized in experiments in which calcite (1 g L^{-1}) and 10 μM Fe(II) were equilibrated for 24 hours, 48 hours or 1 week. The suspension was then sparged with a gas mixture of either 20% CO_2 (80% N_2, v/v) or 100% CO_2, which partly dissolved the calcite particles until the pH stabilized at pH 6.5 or pH 6.0, respectively. Subsamples were taken regularly over the course of the experiments and analyzed after filtration (0.2 μm) for total dissolved Ca^{2+} and Fe(II). Additionally, samples were dissolved in 5 M HCl (Heron et al., 1994; Kostka and Luther III, 1994) to determine total solid iron.

- ***Siderite, an iron (II) carbonate (Partner 16)***

Synthesis

Siderite ($FeCO_3$) was prepared at room temperature and atmospheric pressure similar to the method described by Jönsson and Sherman (2008). 50 ml of 0.2M $Fe(ClO_4)_2$ was drop wise added to 150 ml of 0.3M $NaHCO_3$ in the O_2 free glove box. The pale precipitate formed was transferred to the glove box, allowed to settle during 24 h and then decanted.

During siderite synthesis great care had to be taken to avoid oxidation. In contact with air, the wet paste started to turn orange-brown in a matter of minutes and dried siderite oxidised in a

matter of seconds, evolving considerable amount of heat. When the siderite was allowed to oxidise completely in suspension, goethite was formed.

Characterization

The mineral structure was confirmed by X-ray diffraction.

- ***Se(IV) doped Calcite (Partner 16)***

Synthesis

Synthesis and characterization of Se doped calcite are performed according to Aurelio et al. (2009). Calcite is precipitated in a glove box (P_{O2} < 1 ppm) from supersaturated solutions of calcium carbonate prepared by mixing directly into a reactor two equimolar aqueous solutions (0.5 M) of reagent-grade $CaCl_2$ and Na_2CO_3. All chemicals are reagent grade and used without further purification. Solutions are prepared with Milli-Q (18 MΩ-cm) water. A reference sample of pure calcite is prepared, and 8 samples for which Na_2SeO_3 (SeIV) and Na_2SeO_4 (SeVI) solutions are added to the Na_2CO_3 beaker. The experiments are carried out at 20°C and the precipitates are aged for 2 h and washed 3 times with deionised water in order to eliminate NaCl. Solids are dried and prepared for X-ray and neutron diffraction analyses. Total chemical analyses of the solids are done using an ICP-AES after acid dissolution.

Caracterization

Standard XRD and SEM

Scanning electron microscopy as well as XRD and ND data reveal that under certain conditions the precipitation of calcite is suppressed and other polymorphs of $CaCO_3$ may crystallize, as is the case of vaterite shown in the Figure 1.

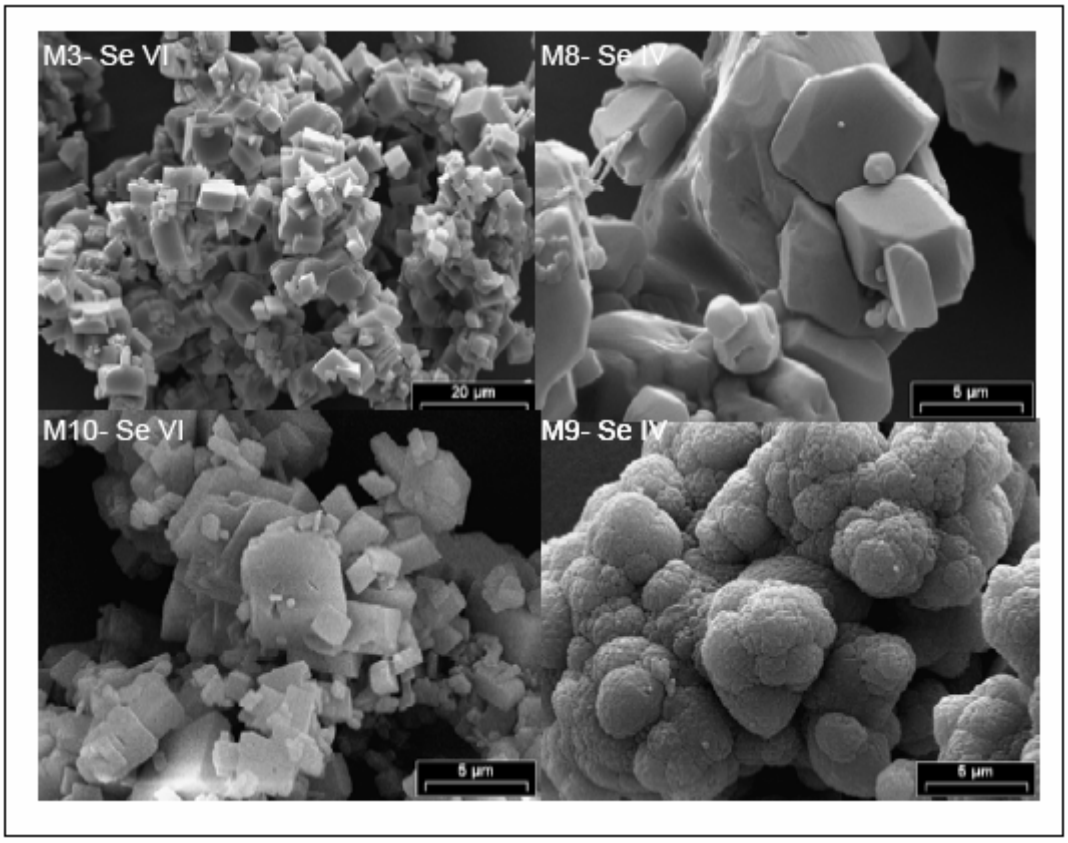

Figure 1. SEM pictures of calcite precipitated in presence of either Se(VI) (left) or Se(IV) (right) (Aurelio et al., 2009)

X-ray Absoption Spectroscopy**.** EXAFS study of local structure X-ray absorption spectroscopy are used to characterize the local structure and coordination of Se(IV;VI) species coprecipitated with calcite from room-temperature aqueous solutions.

EXAFS spectra are collected on selected powdered samples and on aqueous standards at the BM30 beamline of the synchrotron radiation facilities in Grenoble, France (ESRF). Multiple scans are taken for each sample over the Se *K*-edge (12658 eV). Samples are held at near 77 K using a liquid nitrogen cryostat, which improves the signal/noise ratio.

All spectra are calibrated against a selenium metal foil, before summing the scans, using the first inflection point of the spectra. Data analysis proceeds by subtraction of a linear pre-edge background, a second-order polynomial post-edge background, normalization, and conversion to *k*-space, followed by m_0 fitting using a cubic spline. The c(*k*) function is Fourier transformed using k^2 weighting. This data processing is performed using the Athena software.

X-Ray and Neutron Diffraction. Diffraction experiments **.** Powder x-ray diffraction data are recorded on a Philips PW-1700 diffractometer using Cu-*K*a radiation and a graphite monochromator. The collection time in steps of 0.02° was 10 sec. per step. The calibration and alignement of the diffractometer are performed with a CeO_2 standard.

Powder samples are studied at the D20 diffractometer of the Institut Laue-Langevin (ILL) in Grenoble, France. This is a two-axis neutron diffractometer with very high flux. It has a banana-like detector bank composed of 1536 individual micro-strip detectors, covering an

angular range of 150°. The samples are placed in vanadium cylindrical containers and each diffractogram is collected during 60-90 minutes, depending on the amount of sample. The wavelength and zero angle shift are calibrated with a standard Si sample. In this way, the obtained wavelength is 1.306 Å and the zero shift is 0.112°. The collected data are corrected by detector efficiency and normalised by monitor counts.

The measured neutron and X-ray diffraction spectra are processed with the full-pattern analysis Rietveld method, using the program FullProf [FP] for refining the crystal structure. The reference sample of pure calcite is refined assuming the trigonal *R*-3*c* space group with standard atomic positions. Fitted parameters are the lattice constants (*a* and *c*), the *x* coordinate of O atoms and the isotropic thermal constants for each atom.

- ***U(VI) doped calcite (Partner 16)***

Synthesis

To synthesize U(VI)-dope calcite crystals in a glove box (<1 ppm O_2 (v/v)), glass beakers containing an unseeded $CaCl_2/UO_2(NO_3)_2/NH_4Cl$ solution are sealed to the ambient laboratory atmosphere. The CO_3 source, a small open bottle of solid $(NH_4)_2CO_3$ in the beaker allowing only gaseous exchange between $(NH4)_2CO_3$ and the $CaCl_2/NH_4Cl$ solution. $(NH_4)_2CO_3$ decomposes at room temperature forming CO_2 and NH_3 gases that diffuse into the solution. The pH of the solution is controlled by the combination of the acid-base dissociation equilibria for carbonic acid and ammonia resulting in an overall pH increase. The CO_2 ultimately yields CO_3^{2-} and HCO_3^- which react with dissolved Ca^{2+} to precipitate $CaCO_3$.
The initial pH of the growth solution was measured. The detailed reaction conditions are listed in Table-1. The calcite nucleation occurred within 1-4 days depending on initial Ca^{2+} concentration. After nucleation of calcite crystals, the pH was measured and the CO_3 source was removed. Then U(VI) (as 1000 ppm $UO_2(NO_3)_2.6H_2O$ solution) were added. During the course of the experiments pH and the total CO_2 concentrations (as total alkalinity) were measured daily. U concentration in solution was measured by ICP-AES at the end of the experiments. After removal of the CO_3 source, the free-drift experiments represent a closed system resulting in depletion of Ca^{2+}, total CO_2, UO_2^{2+} during calcite growth. The experiments were terminated 3-5 days after nucleation and calcite single crystals were rinsed with deionised water (18 MΩ Millipore), and dried at 60^0 C prior to analysis.

Table-1: Reaction conditions of U rich calcite co-precipitation

Expt	[Ca(II)] (mmol/kg)	pH initial	ΣCO_2 (mmol/kg)	[Fe(II)] (mmol/kg)	[Se(IV)] (mmol/kg)	[U(VI)] (mmol/kg)	$SI_{schoepite}$	$SI_{siderite}$	$SI_{calcite}$
U	10-15	7.5	10-15	0.01-0.05	-	(a) 4×10^{-3} (b) 4×10^{-2}	(-7.5) - (-6.5)	0.35-1.05	1.24

SI values calculated using MINTEQA2

Characterization

The solids will be characterized by X-Ray diffraction and EXAFS spectroscopy.

1.2.2 Sulfates

- ***Phosphogypsum (Partner 20)***

Material origin

Phosphogypsum is the by-product of the phosphoric acid industry and is obtained by reacting phosphate rock with sulfuric acid. From the beginning of 80's to the mid of 90's, approximately 300 000 tons of phosphogypsum have been produced by a former phosphate fertilizer industry in Cyprus and stockpiled onto a coastal area of about 50 000 m^2. The disposal site (about 50 000 m^2) can be distinguished into three sub-areas determined by the age of phosphogypsum and its composition. Area 1 and 2 are characterised by aged and non-aged phosphogypsum, respectively. Area 3 differs from the other stacks by receiving large amounts of seawater, which covers the area in winter and evaporates in summer leaving behind its salt content. On the different sub-areas there have been drilled monitoring/probing wells into the stack and phosphogypsum samples were obtained every meter, and stack solutions were sampled at a well depth of 5 meters.

Characterization

Physical characterisation of phosphogypsum included density measurements, water content analysis, mineralogical composition by X-ray diffraction (XRD-6000) and was performed on non-treated samples. The water content has been determined using thermogravimetric analysis (TGA-50) by drying phosphogypsum samples up to 800 °C at constant temperature gradient (10 degrees/min). The free water content of the samples was calculated by subtraction of the hydration water from the total water release. On the other hand, compositional and radiochemical characterisation was carried out with samples which were prepared by grinding (to a grain size less than 500 μm, 30 mesh) and drying the powders at 100 oC under atmospheric conditions. The composition of the phosphogypsum samples was determined by ED-XRF and carbon/sulfur analysis (CS-800), whereas radiochemical characterisation included gamma measurements carried out by high resolution semiconductor detection systems (HPGe detectors) and solid scintillation detectors (NaI(Tl) detector). The physicochemical characteristics and the uranium content of the stack solutions were determined using standard classical (wet-chemistry) methods, instrumental methods (ICP-OES and Ion-Chromatography HPLC) and radiometric methods of analysis (alpha-spectrometry).

The bulk density of phosphogypsum samples investigated in this study ranged between 1.4 and 1.7 g cm^{-3}. The hydration water content is almost constant (19% ± 2 %), whereas the free water content is varying between 1% and 25%, with samples from Area 1 having the lowest (1 - 2%) and samples from Area 3 the highest (up to 25%) water content.

Although the sensitivity of X-ray diffraction is not sufficient to determine compounds at trace levels some crystalline materials included in phosphogypsum such as quarz, clays, iron (oxo)hydroxides and sodium chloride could be identified. Moreover, X-ray diffraction measurements clearly showed that the top of the aged phosphogypsum consisted mainly of calcium carbonate (calcite) and phosphogypsum adjacent to sea included increased amounts of quartz, clays and sodium chloride, resulting from seawater inputs. The latter is supported

also by ED-XRF measurements. Table 2 summarizes major element composition (%) and trace element concentration of phosphogypsum samples obtained from the stack in Cyprus.

Table 2. Average major element composition (%) and trace element content (ppm) of Cyprus phosphogypsum

species	CaO	SO_3	P_2O_5	SiO_2	Fe_2O_3	Al_2O_3	H_2O (hydr.)
%	31.0	42.0	0.02	0.3	0.05	0.2	19
trace	Ba	Zn	Cl				
ppm	3 - 100	1 - 22	40 - 500				

Table 3. Radioactivities of key radionuclides in Cyprus phosphogypsum

	Radionuclide / (Bq kg^{-1})		
sample	**U-238**	**Ra-226**	**Th-232**
Phosphogypsum *average (max-min) value*	85 (330-21)	723 (1053-428)	37 (62-4)

Table 4. Composition of the main constituents (mean values) in the stack solutions from three different areas of the Vasiliko phosphogypsum stack.

Borehole	**Area 1**	**Area 2**	**Area 3**
pH	4.3	2.4	2.6
EC (uS)	9507	35100	57300
anions in mg/l			
$[Cl^-]$	1416	8828	16300
$[SO_4^{2-}]$	2622	3857	6730
$[NO_3^-]$	262	2881	76
$[PO_4^{3-}]$	875	1864	277
$[F^-]$	17	176	35
cations in mg/l			
$[Na^+]$	1098	6308	9125
$[Ca^{2+}]$	862	211	1500
$[Mg^{2+}]$	113	1134	1134
$[K^+]$	82	253	1500
[U] in ug/l	2	81	282

1.2.3 Sulfides

- ***Mackinawite Nanoparticles (Partners 16 and 22)***

Synthesis

Experiments were run under O_2-free glove box and all the solutions were prepared from Milli-Q water, purged for at least 30 min with O_2-free argon before use. Fe(II) sulphides were precipitated from $FeCl_2$,$4H_2O$ or $FeSO_4$,$7H_2O$ and Na_2S, 8–$9H_2O$ solutions, according to Wolthers et al. (2003, 2005). The precipitates were obtained at room temperature by mixing 100 mL of the Fe(II) solution with 100 mL of the Na_2S solution. The Fe(II) concentration in the resulting 200 mL was set at 0.1 mol L^{-1} this study. Only the Na_2S concentration was varied and the results are then given as functions of the concentration ratio Fe/S = [Fe(II)]/[S(-II)] = [$FeCl_2$ or $FeSO_4$]/[Na_2S]. Ratios ranging from ½ to 2 were considered. The precipitates were analysed after 3 days to 3 months months of ageing times at room temperature in anoxic conditions. Once the formation of the precipitate was achieved, the whole suspension was poured in a flask. The flask was completely filled with the suspension and sealed carefully to avoid infiltration of air. During the ageing period, the suspension was kept static.

Characterization

The size of the partyicle was obtained by the Pair Distribution Function (PDF) based on High Energy X-Ray Diffraction measurements performed in Grenoble.

Finely powdered dry samples of pure mackinawite were loaded into 0.8 mm diameter polymide capillaries and sealed with wax under anoxic conditions ([O2]<2 ppm) in a constant-flow N_2 glove-box. High-energy X-ray total scattering data acquisition was performed at beamline ID15B of the European Synchrotron Radiation Facility, Grenoble, France. Scattering data were collected with a Pixium 4700 flat-panel detector using the Rapid-Acquisition Pair Distribution Function technique (Chupas et al., 2003). Samples, an empty capillary and the background were measured at ambient temperature from 0–23.2 $Å^{-1}$. The X-ray wavelength was refined using a Ni standard (λ=0.14134 Å). Corrections for sample-detector distance, tilt angle of the detector with respect to the direction of the incident radiation and polarization were performed using Fit2D (Hammersley et al., 1996; Hammersley, 1998). Total scattering structure functions and Pair Distribution Functions (PDF) were obtained using the PDFGetX2 software (Qiu et al., 2004). A crystalline standard (LaB6) was measured and used to estimate the instrumental resolution effect on the PDF (Toby and Egami,1992). Fits of the PDFs were performed using the PDFGui software (Farrow et al., 2007).

Fig. 2 shows the PDF of mackinawite. The fast decay of the samples indicates an additional effect of a finite coherent domain size. Using σQ of LaB6 as fixed parameter, the domain size parameter, Sp, of mackinawite was fitted, resulting in 5.2 nm. These values correspond to mean particle sizes assuming spherical particles. The specific surface area calculated from this particle size is 270 m^2/g. PDF analysis of a freshly precipitated mackinawite showed a particle size of 2 nm, which increased with aging to 4–5 nm (Michel et al., 2005). Using high resolution transmission electron microscopy, laminar rectilinear prisms with 2 to 5.7 nm in thickness and 3 to 10.8 nm in length were observed for a similar sample (Ohfuji and Rickard, 2006). Therefore, PDF-derived and TEM-derived particle sizes are in good agreement.

The close fit of the experimental spectra based on single unit cells of mackinawite (Lennie et al., 1995), as well as the fitted unit cell parameters imply that the structures of the nanoparticles are very similar to the respective crystalline phases. Surface relaxation and other structural effects, which might occur for nanosized particles, were hence not observed.

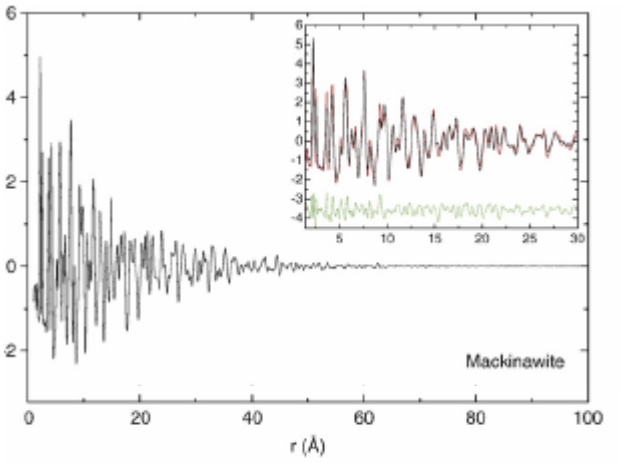

Figure 2. Pair Distribution Function (PDF) analysis of high-energy X-ray total scattering data for mackinawite nanoparticles. Fits of the local structure of mackinawite models are shown in the insets (red: experimental data; black: fit; blue: residual) (Scheinost et azl., 2008)

- ***Pyrrhotite (Partners 6 and 7):***

Both natural and synthetic pyrrhotite will be used in the experiments to compare the different redox behaviour of the materials according to their nature.

Pyrrhotite is the most common iron sulfide in nature, after pyrite, and shows a non-stoichiometric composition as $Fe_{1-x}S$ where x varies from 0 (FeS) to 0.125 (Fe_7S_8). The formula can also be expressed as $Fe_{n-1}S_n$ with $n \geq 8$ to give structures from Fe_7S_8 to $Fe_{11}S_{12}$. Because of its sulphidic nature, pyrrohotite can experiment oxidation, in both sulphur and iron ions.

Pyrrhotite has been selected as test material due to the relevance of sulfides in radionuclide retention processes and because its less studied than pyrites.

Synthesized pyrrhotite: Synthesized pyrrhotite will be hydrothermally prepared according to reference [1]. 4.5 ml of 0.6 M Mohr's salt solution will be mixed with 4.5 ml of 1.2 M Na_2S solution in a Pyrex tube at room temperature. The tube will be sealed and autoclaved in a silicon oil bath at 200ºC heating for 5 hours. Dark-brown particles will form in the solution. Synthesized pyrrhotite will be crushed and sieved to particle size: 100-150 microns. Solid identification will be done by X-Ray diffraction and particles will be examined by SEM. Specific surface area will be determined by the BET method.

Natural pyrrhotite:
Natural pyrrhotite was obtained from Gualba, located in Catalonia, Spain.

In its mineralogical composition, apart from pyrrhotite, small quantities of quartz and pyrite have been identified.

Samples will be crushed and sieved to work with grounded powder with a particle size in the range of 100-150 μm.

As a general pre-treatment, in all cases fines from the crushing procedure will be eliminated by rinsing with ethanol prior to the start of experiments, including the characterisation.

The sample presents thin oxide layers covering the surface that will be removed during grounding preparation under ethanol and subsequence etching in ethanol in the ultrasonic-bath. Powder sample will be kept under nitrogen atmosphere to prevent further oxidation.

- ***Pyrite (Partners 3 and 16)***

Origin, purity and electric conductivity

The two samples to be used originate from Spain and Peru. They are of good chemical purity (96%) (see table I for electron microprobe analysis) but their electric conductivities are quite different: pyrite from Spain is about 1000 times more conductive than that from Peru. Previous studies showed that despite the dramatic difference in the electric conductivity of massive samples their reactivity is quite similar if pyrite is reduced into micrometric particles. Conductive samples are used to perform voltammetric experiments or to visualize local corrosion phenomena by the measurement of the local galvanic activity. On the other hand, when dielectric techniques are applied, the use of bad conducting samples allows the detection of the formation of conductive species on the pyrite surface and, conversely, the use of well conducting samples allows the detection of insulating ones. XRD patterns are in agreement with the expected ones.

Element	**Co** %	**Cu** $g.t^{-1}$	**Ni** $g.t^{-1}$	**Fe** %	**S total** %	**SO_4** %	**S_2^{2-}** %	**S^0** %
Concentration	< 0,01	2715	16	45,10	51,60	1,90	50,90	0,06

Table 5. - Chemical analyses by AAS of a pure pyrite from Peru.

Element	**SiO_2** %	**Al_2O_3** %	**CaO** %	**MgO** %	**K_2O** %	**MnO** %	**TiO_2** %	**P_2O_5** $g.t^{-1}$	**Li** $g.t^{-1}$	**Be** $g.t^{-1}$	**B** $g.t^{-1}$	**V** $g.t^{-1}$	**Cr** $g.t^{-1}$	**Zn** $g.t^{-1}$
Concentration	0,95	< 0,01	< 1,00	< 1,00	< 0,50	< 0,01	< 0,01	-	< 10	< 2	< 26	85	12	20
Element	**As** $g.t^{-1}$	**Sr** $g.t^{-1}$	**Y** $g.t^{-1}$	**Nb** $g.t^{-1}$	**Mo** $g.t^{-1}$	**Ag** $g.t^{-1}$	**Cd** $g.t^{-1}$	**Sn** $g.t^{-1}$	**Ba** $g.t^{-1}$	**La** $g.t^{-1}$	**Ce** $g.t^{-1}$	**W** $g.t^{-1}$	**Pb** $g.t^{-1}$	**Bi** $g.t^{-1}$
Concentration	438	22	< 20	< 20	< 5	12,3	< 2	240	< 10	< 20	< 10	1101	< 10	515

Table 6. - Chemical analyses by ICP of a pure pyrite from Peru.

Characterization

Mineralogical composition

The determination is made by x-rays diffractometry using a Siemens D 5000 equipment. The operating conditions are the following: scanning from 4 to 84° 2θ at a rate of 0,02° 2θ s-1. The treatment of the spectra is done using the Diffrac AT software. The results show the exclusive presence of pyrite. No other phase could be highlighted.

Particle size, surface area and site density

The study of the reactivity of pyrite with various reagents is performed using powders in the 40-80 µm size range in the presence or not of pyrite plates. During the stirring of the suspensions the particles size diminishes because the attrition. Therefore, after 2 weeks of stirring, the particles of a 40-80 µm initial suspension are smaller than 20 µm. The surface areas determined for pyrite, 0.13 m^2/g for particles in the 40-80 µm range and 0.8 m^2/g for particles smaller than 20 µm, are in the range of values reported in the literature (fig. 1). Regarding the site density the published data are not so many and vary from 3.7 to 12 sites/nm^2 according to the method used for their determination (fig. 1).

Grinding, pretreatment, oxidation prevention

Pyrite suspensions are prepared by manual dry grinding millimetric (2-3 mm) lumps just before use, then, the experiments are performed under argon atmosphere or under vacuum in sealed glass tubes. This way to proceed strongly limits the oxidation by air as it is proved by voltammetric and XPS characterizations. Moreover, because the attrition of pyrite particles the reactants are in contact with a fresh pyrite surface. It is the same when pyrite plates are in the presence of suspensions.

Working hypothesis related to pyrite

In several studies on the underground storage of spend nuclear fuel, it is accepted that small amounts of pyrite (~1 wt %) are responsible for the low redox potential of geological environments planned for the storage of the spent fuel. For this reason it is important to obtain data on the evolution of pure pyrite in the presence of oxidizing radionuclides before to consider the reactions in Callovo-Oxfordian argillite. The literature is poor in the area of interactions of pyrite with uranium, selenium and iodine soluble species and, to our knowledge, there are neither bibliographic references concerning the reactivity of their mixtures towards this mineral, nor studies performed by means of voltammetric techniques on this subject.

In previous studies we have shown that the global reactivity of pyrite towards mixtures, i.e. Ag(I) and Hg(II), can be very different from the individual contributions! For example the amount of mercury fixed by pyrite is not influenced by the presence of silver in solution. On the contrary, the presence of mercury excludes the sorption of silver. On the other hand pyrite that reacted beforehand by silver can fix more mercury than pure FeS_2.

1.2.4 Oxy(hydroxy)des

- ***Goethite and Hematite (Partners 6 and 7)***

Goethite and hematite were obtained from the deposit of Cerro del Hierro, located in Sevilla, Spain. This deposit consists of clays and iron oxides that fill palaeo-karsts in Cambrian limestones.

Both samples had been characterised by DRX (Figures 3 and 4) and the spectra detect iron oxides and SiO_2. In the hematite sample, impurities of goethite had been also identified.

BET determined surface area for 0.25 mm average particle size were 2.01±0.01 $m^2 \cdot g^{-1}$ for goethite and 0.38±0.01 $m^2 \cdot g^{-1}$ for hematite. New fraction range 100-150 µm particle size will be prepared and surface area measured again.

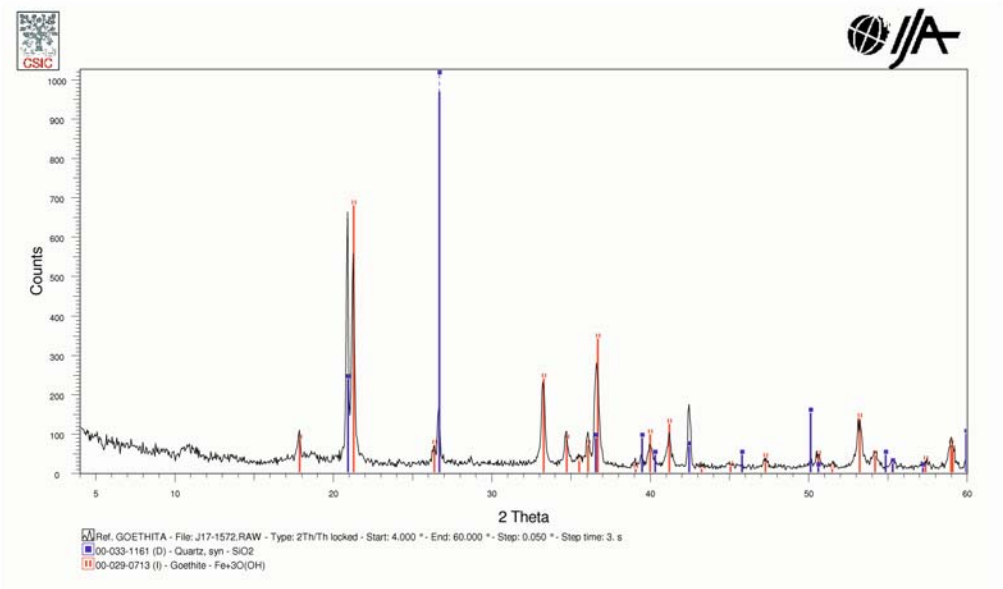

Fig 3. DRX spectra for natural goethite.

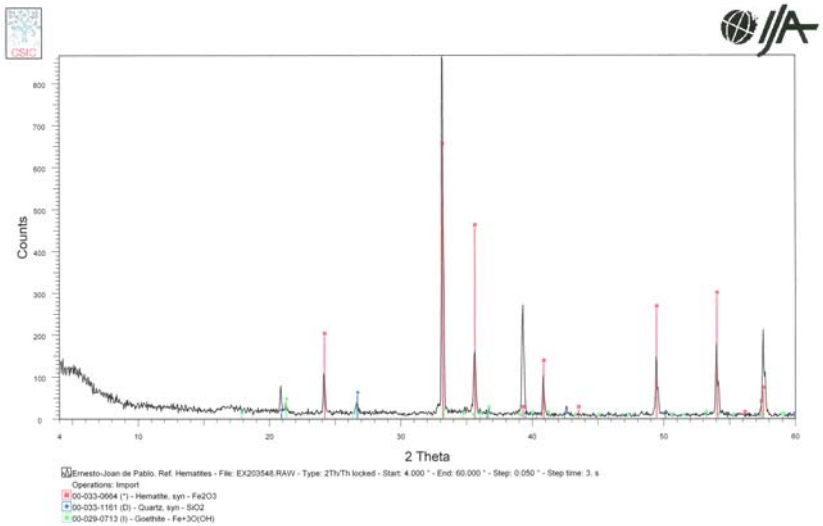

Fig 4. DRX spectra for natural hematite.

- ***Lepidocrocite (Partner 22)***

Synthesis.

The lepidocrocite sample has been synthesized according to Cornell and Schwertmann (2000).

Characterization

The X-Ray diffraction spectrum is given below (Figure 5).The BET surface area was determined to be of 78 m^2/g.

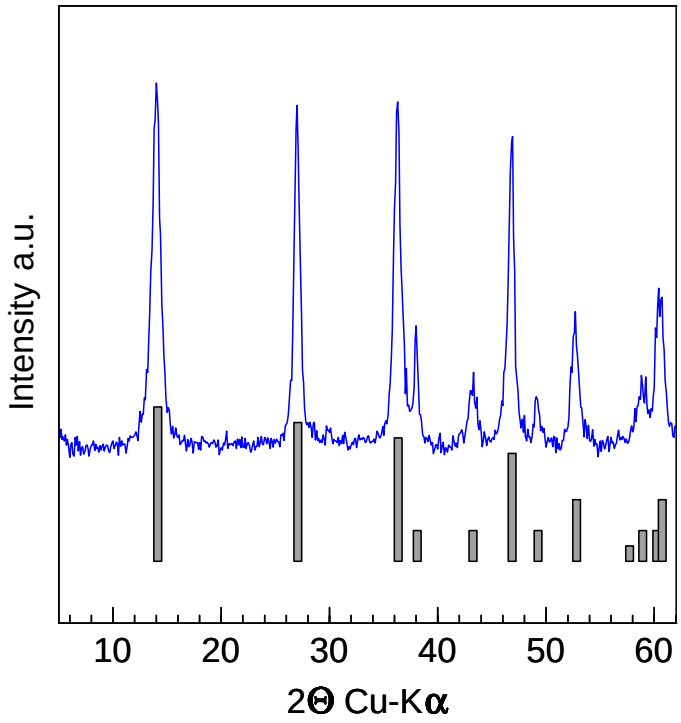

Figure 5 X-ray diffractogramm of lepidocrocite used by UNIUTR. The gray bars indicate the characteristic diffractions of lepidocrocite.

- ***Magnetite (Partners 6 and 7)***

Natural magnetite comes from the deposit of Kiruna, in Sweden.

The Fe(II)/Fe(III) ratio from XPS determinations match with a pure magnetite content.

Measured BET of a 0.1 mm particle size fraction gives surface area of 0.89±0.01 $m^2 \cdot g^{-1}$. New sample of 100-150 μm particle size will be prepared and surface area will be measured afterwards.

Raw natural iron oxides samples can be considered stable in the time frame of the experiments and no especial actions will be taken regarding to oxidation prevention before preparation of powder samples. However, grounded samples will be kept under nitrogen atmosphere to prevent any risk of alteration.

1.2.5 Claystone

- ***Boda Claystone sample (Partner 19***)

The rock sample materials used in WP3 by II-HAS are borecores from the Boda Claystone. Samples are originated from two boreholes – one drilled from the ground, the other drilled from a shaft in a depth of ~ 1000m.

Thin slices (discs with ~ 8 mm thicknesses) as well as grounded powders shall be used. (The slices are used also in WP 5 for through diffusion studies.)

The particular feature of the two series of samples is that they are selected from regions where an interception of a thin transient stratum formed under reducing environment is found in the borecore. (The conditions during the formation of the overwhelming part of the Boda Claystone were oxidizing – the occurence of a stratum formed under reducing conditions is exceptional.)

A typical mineral composition of the Boda Claystone (formed at oxidative conditions) is : Illite-muscuscovite 38 %, albite 30 %, quartz 8 %, hematite 9 %, chlorite 6 %, dolomite 5 %, calcite 4 %. The mineral composition in the reduced stratum is different : illite-muscovite 25 %, albite 27 %, quartz 12 %, chlorite 18 %, calcite 3 %, dolomite 1 %, there is no hematite in detectable amounts, and a new component, kaolinite appears in 10 % .

The working hypothesis is based on the comparison of the behaviour of the different strata. Samples originated from the different zones are planned to be exposed to controlled redox treatments and their responses (derived mostly from the change of the Fe^{2+}/Fe^{3+} ratio determined by Mössbauer spectroscopy; See Figure 6) are to be compared.

(It should be noted that there was no special care taken to prevent the exposure of the samples to air during storage. Hovewer, the samples originated from the reduced stratum hardly display any effects of oxidation (at least as detected by Mössbauer spectroscopy – prepondering part of iron in this sample is Fe^{2+}, whereas the other samples originated from the common prepondering parts of the formation contain Fe^{3+} in ca. 95 % portion of iron.)

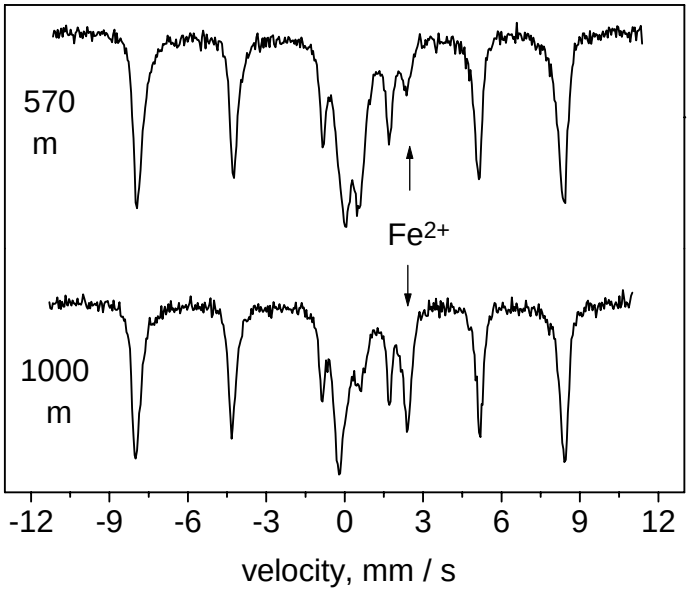

Figure 6 *Mössbauer spectra of the iron bearing components of Boda Claystone samples. The main component is hematite (sextet), the peak marked with Fe^{2+} belongs to chlorite.*

- ***Callovo Oxfordian argillite - COx (Partners 3 and 16***)

A Callovo-Oxfordian argillite (COx) core (1 m in length) will be sent by ANDRA to CEA. CEA will forward sub-samples (cut in anoxic glove box) to each partner in anoxic plastic bags. BRGM, that has long time experience with COx, is going to sent previous characterization results.

The characterization of the argillite that will be used is fully reported in three papers (Tournassat et al., 2008; Gaucher et al., 2006; 2004), as well as in the FUNMIG European Programme Final Report (Altman et al., 2008).

Physical property measurements (water content, porosity, density, specific surface), geochemical analyses (major and trace elements, cation exchange capacity [CEC] and surface cation occupancy, leaching anions, redox state, organic matter concentration), and a semi-quantitative mineralogical study were conducted on the samples. All the steps of the sampling and of the characterisation are done with a research of limitation of the oxidation to obtain representative samples of the in situ conditions. The top of the formation is more carbonate-rich, with interbedded clayey layers and carbonate rock. The formation is more homogeneous in its central section with a clay mineral concentration of 45–50%, which corresponds to a maximum of flooding within the area. In the upper part of this section, micas and mixed-layer illite/smectite R0 dominate, whereas in the lower part of the section we find an abrupt transition to mixed-layer illite/smectite R1 associated with kaolinite.

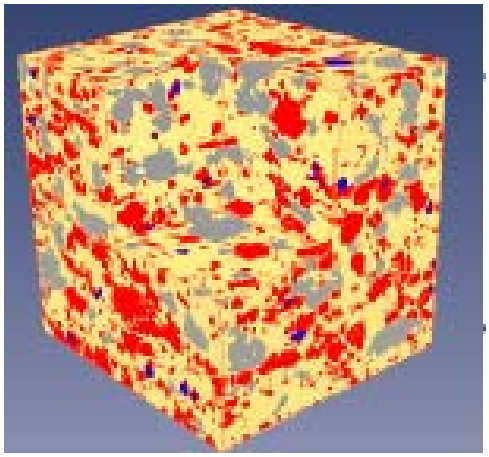

Figure 7. COx X-Ray tomgraphy of a 200 μm large argillite cubic sample (Altman et al., 2008)

2. References

- Altman S. (2008) RTDC 3&1, FUNMIG Final Report
- Aurelio, G., Fernández-Martínez, A. , Cuello, G. J., Román-RossG. , Ialliot, I. , Charlet L. (2009) Structural study of substitution in calcite (in prep.)
- Bourdoiseau J.-A., Jeannin M., Sabot R., Rémazeilles C., Refait Ph. 2008. Characterisation of mackinawite by Raman spectroscopy. Corrosion Science 50, 3247–3255.
- Cheng L., Lyman P. F., Sturchio N. C., Bedzyk M. J., 1997. X-ray standing wave investigation of the surface structure of selenite anions adsorbed on calcite Surf. Sci. 382, L690.
- Cornell and U. Schwertmann (2000) "Iron oxides in the Laboratory", Wiley-VCH
- Elzinga, E.J., Tait, C.D., Reeder, R.J., Rector, K.D., Donohoe, R.J., and Morris, D.E., 2004. Spectroscopic investigation of U(VI) sorption at the calcite-water interface. Geochim. Cosmochim. Acta 68, 2437-2448.
- Gaucher E., Robelin C., Matray J.M., Negrel G., Gros Y., Heitz J.F., Vinsot A., Rebours H., Cassagnabere A., Bouchet A. (2006) ANDRA underground research laboratory: interpretation of the mineralogical and geochemical data acquired in the Callovian–Oxfordian formation by investigative drilling. C. R. Geoscience 338 (917–930.
- Gaucher É.C., Blanc P., Bardot F.,. Braibant G., Buschaert S., Crouzet C., Gautier A., Girard JP., Jacquot E., Lassin A., Negrel G., Tournassat C., Vinsot A., Altman S. (2004) - Modelling the porewater chemistry of the Callovian–Oxfordian formation at a regional scale. Physics and Chemistry of the Earth 29 55–77.
- Giménez, J., M. martínez, J. de Pablo, M. Rovira, L. Duro.(2007) Journal of Hazardous materials, 141, 575-580.
- Horiuchi, Shigeo; Wada, Hiroaki. (1971)Two-dimensional superstructure in hydrothermally synthesized pyrrhotite. Acta Crystallographica, Section B: Structural Crystallography and Crystal Chemistry, 27(2), 504-5.
- Jönsson J., Sherman D.M. (2008) Sorption of As(III) and As(V) to siderite, green rust (fougerite) and magnetite: Implications for arsenic release in anoxic groundwaters. Chemical Geology 255, 173–181.
- Lamble, G.M., Lee, J.F., Staudt, W.J., and Reeder, R.J., 1995. Structural studies of selenate incorporation into calcite crystals. Physica B, 208/209, 589-590.
- Martínez, J. Giménez, J. de Pablo, M. Rovira, L. Duro.. Sorption of selenium (IV) and selenium (VI) onto magnetite. Applied Surface Science, (2006), 252, 3767-3773.
- Mettler S., Wolthers M., Charlet L., von Gunten U. (2009) Sorption and catalytic oxidation of Fe(II) at the surface of calcite Geochimica et Cosmochimica Acta (in press).
- Reeder, R.J., Lamble, G.M., Lee, J-F., and Staudt, W.J., 1994. Mechanism of SeO42- substitution in calcite: An XAFS study. Geochim. Cosmochim. Acta, 58, 5639-5646.
- Reeder, R.J., Nugent, M., Lamble, G.M., Tait, C.D., and Morris, D.E. (2000) Uranyl incorporation into calcite and aragonite: XAFS and luminescence studies. Environ. Sci. Tech., 34, 638-644.
- Reeder, R.J., Nugent, M., Tait, C.D., Morris, D.E., Heald, S.M., Beck, K.M., Hess, W.P., and Lanzirotti, A., 2001. Coprecipitation of uranium(VI) with calcite: XAFS, micro-XAS, and luminescence characterization. Geochim. Cosmochim. Acta, 65, 3491-3503.
- Rovira, J. Giménez, M. martínez, X. Martínez-Lladó, J. de Pablo, V. Martí, L. Duro.. Sorption of selenium (IV) and selenium (VI) onto natural iron oxides: goethite and hematite. Journal of Hazardous materials, (2008), 150, 279-284.
- Staudt, W.J., Reeder, R.J., and Schoonen, M.A.A., 1994. Surface structural controls on compositional zoning of SO42- and SeO42- in synthetic calcite single crystals. Geochm. Cosmochim. Acta, 58, 2087-2098.
- Tournassat C., Lerouge C. Blanc P., Brendle J. Greneche JM., Touzelet S., E.C. Gaucher (2008) - Cation exchanged Fe(II) and Sr compared to other divalent cations (Ca,Mg) in the bure Callovian–Oxfordian formation: Implications for porewater composition modelling. Applied Geochemistry 23 (2008) 641–654.
- Wolthers M., Charlet L., Van der Linde P.R., Rickard D., Van der Weijden C.H. (2005) The surface chemistry of disordered mackinawite Geochim. Cosmochim Acta 69 (14): 3469-3481.
- Wolthers et al. (2003), American Mineralogist, Volume 88, pages 2007–2015.